International Conference on Space Optics—ICSO 2006

Noordwijk, Netherlands

27–30 June 2006

Edited by Errico Armandillo, Josiane Costeraste, and Nikos Karafolas

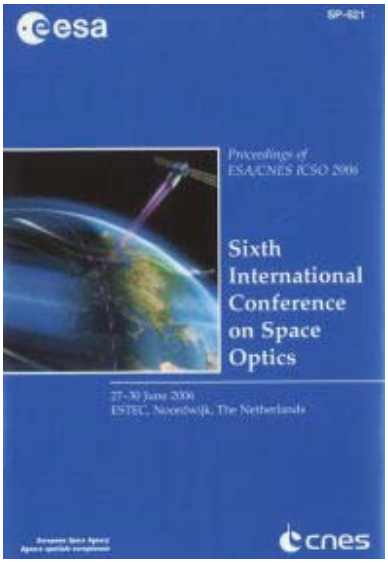

A heterodyne interferometer for high resolution translation and tilt measurement as optical readout for the LISA inertial sensor

Thilo Schuldt, Hans-Jürgen Kraus, Dennis Weise, Claus Braxmaier, et al.

International Conference on Space Optics — ICSO 2006, edited by Errico Armandillo, Josiane Costeraste, Nikos Karafolas, Proc. of SPIE Vol. 10567, 105673M · © 2006 ESA and CNES
CCC code: 0277-786X/17/$18 · doi: 10.1117/12.2308065

A HETERODYNE INTERFEROMETER FOR HIGH RESOLUTION TRANSLATION AND TILT MEASUREMENT AS OPTICAL READOUT FOR THE LISA INERTIAL SENSOR

Thilo Schuldt[1,2], Hans-Jürgen Kraus[1,2], Dennis Weise[1], Claus Braxmaier[1,3], Achim Peters[2], and Ulrich Johann[1]

[1] *EADS-Astrium GmbH, Claude-Dornier-Straße, 88039 Friedrichshafen, Germany, E-mail: dennis.weise@astrium.eads.net*
[2] *Humboldt-Universität zu Berlin, Hausvogteiplatz 5-7, 10117 Berlin, Germany, E-mail: thilo.schuldt@physik.hu-berlin.de*
[3] *Hochschule für Technik, Wirtschaft & Gestaltung, Brauneggerstr. 55, 78462 Konstanz, Germany, E-mail: braxm@fh-konstanz.de*

ABSTRACT

The space-based gravitational wave detector LISA (Laser Interferometer Space Antenna) requires a high performance position sensor in order to measure the translation and tilt of the free flying test mass with respect to the LISA optical bench. Here, we present a mechanically highly stable and compact setup of a heterodyne interferometer combined with differential wavefront sensing for the tilt measurement which serves as a demonstrator for an optical readout of the LISA test mass position. First results show noise levels below $1\,\mathrm{nm}/\sqrt{\mathrm{Hz}}$ and $1\ \mu\mathrm{rad}/\sqrt{\mathrm{Hz}}$, respectively, for frequencies $> 10^{-3}\,\mathrm{Hz}$.

1. INTRODUCTION

Planned to be launched around 2015 the NASA/ESA collaborative mission LISA (Laser Interferometer Space Antenna) aims at detecting gravitational waves in the frequency range $30\,\mu\mathrm{Hz}$ to $1\,\mathrm{Hz}$. With a strain sensitivity of $3.2 \cdot 10^{-19}$ at a frequency of $10^{-3}\,\mathrm{Hz}$ it will detect gravitational waves caused e. g. by neutron star binaries, white dwarf binaries, super-massive black hole binaries and super-massive black hole formations.

The LISA mission consists of three identical spacecraft which form an equilateral triangle in a heliocentric Earth-trailing orbit, approx. 20° behind the Earth (cf. Fig. 1). Any combination of two arms of the LISA triangle forms a Michelson interferometer with an armlength of about 5 mio. kilometers. Gravitational waves passing the LISA formation will be measured as changes in the length of the interferometer arms by use of laser interferometry with $\sim 10\,\mathrm{pm}/\sqrt{\mathrm{Hz}}$ accuracy. Two free flying test masses on each satellite represent the end mirrors of the interferometer. Additionally, one of the test masses acts as inertial reference for the satellite orbit. In the current baseline design, the laser light coming from the distant spacecraft is not directly reflected by the test mass, but the (heterodyne) beat signal with the local oscillator is measured on the optical bench. In addition, the distance between optical bench and its associated test mass has to be measured with the same accuracy as in the distant spacecraft interferometry. In this so-called strap-down architecture, the LISA test mass position sensor is part of the so called science interferometer and must fulfill requirements of $5\,\mathrm{pm}/\sqrt{\mathrm{Hz}}$ (for frequencies above 2.8 mHz with an f^{-2} relaxation down to $30\,\mu\mathrm{Hz}$) for the translation measurement and at least $20\,\mathrm{nrad}/\sqrt{\mathrm{Hz}}$ for the tilt measurement (for frequencies above 0.1 mHz with an f^{-1} relaxation down to $30\,\mu\mathrm{Hz}$). These requirements necessitate an optical readout of the test mass position utilizing laser interferometry for the LISA sensitive axes.

1.1. Drag-Free Attitude Control System (DFACS)

External disturbances like solar radiation pressure or solar wind will change the position of the spacecraft and thereby might affect the interferometer signals caused by gravitational waves. Therefore, a free-flying test mass inside the satellite is taken as reference for a purely gravitational orbit of the satellite. As the external disturbances only act on the surface of the satellite, the distance between the test mass and its housing (which is rigidly connected to the satellite) is changing. In case of a drag-free controlled satellite, any change of the test mass position is measured and the satellite is controlled in such a way that it is centered around the test mass at

Proc. '6th Internat. Conf. on Space Optics', ESTEC, Noordwijk, The Netherlands, 27-30 June 2006 (ESA SP-621, June 2006)

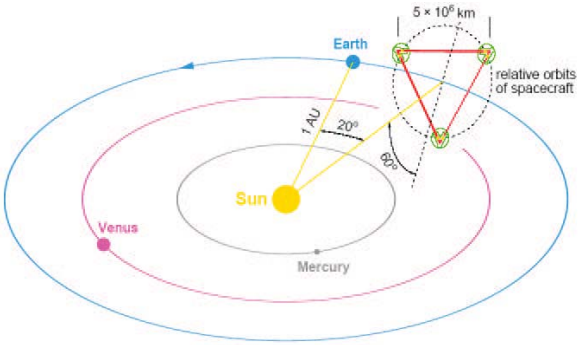

Figure 1. The three LISA spacecraft are flying in a heliocentric orbit, 20° behind the Earth. (In this schematic, the LISA triangle is enlarged by a factor of 10).

any time, cancelling all non-gravitational forces acting on the spacecraft (drag-free attitude control system, DFACS). The actuation of the satellite is done by miniaturized ion engines as part of the so-called μ-propulsion system.

In case of LISA, the test mass is a 46 mm cube made of a gold-platinum alloy. Its surrounding housing includes all electrodes needed for a capacitive readout. This readout provides the translation and tilt information of the test mass with respect to the housing, i. e. the input signals for the drag-free control feedback loop. The requirements for the LISA DFACS position sensor are $< 1\,\mathrm{nm}/\sqrt{\mathrm{Hz}}$ for the translation measurement and $< 20\,\mathrm{nrad}/\sqrt{\mathrm{Hz}}$ for the tilt measurement, both for frequencies down to 0.1 mHz. Current baseline concept for this purpose is the use of a capacitive readout, an optical readout can support this sensor with respect to noise performance and redundancy.

1.2. Optical Readout for the Test Mass Position Measurement

In general, various methods for a LISA inertial sensor optical readout ar conceivable, e. g. :

- lever sensor, i. e. sensing of the test mass position via position sensitive photodiode (e. g. CCD),
- single-path interferometer: Michelson (or Mach-Zehnder) interferometer with the test mass in one of its arms,
- multiple-path interferometer: use of optical resonators with one of the mirrors rigidly connected to the test mass (or coated test mass).

The first method is under investigation at the University of Napoli (Italy). They demonstrated a displacement noise below $10^{-9}\,\mathrm{m}/\sqrt{\mathrm{Hz}}$ for frequencies $> 10^{-2}$ Hz [1]. A tilt of the test mass is measured by reflecting the light twice on the test mass before hitting a quadrant photodiode. This method can presently not provide the sensitivity needed in the LISA science interferometer but can serve as position sensor for DFACS, supporting the capacitive readout.

Michelson and Mach-Zehnder interferometers are state of the art technologies which are highly developed in a variety of different implementations. Such interferometers offer pm-accuracy – demonstrated in lab experiments. A tilt measurement can be implemented by performing a spatially resolved phase measurement, e. g. with quadrant photodiodes (Differential Wavefront Sensing, DWS [2],[3]).

The use of optical resonators (cavities) is most promising, providing the highest sensitivity in position sensing: $1\,\mathrm{fm}/\sqrt{\mathrm{Hz}}$ by use of 1 μW laser power and a resonator finesse of 100. A further increase in finesse by a factor of 1000 will give a – theoretical – sensitivity of 1 am. A tilt of the test mass might be measured by analyzing higher order modes in the cavity. This technology is not yet demonstrated in a lab experiment and is also highly complex (use of several lasers, which are frequency stabilized to several cavities).

Single path interferometers can either utilize one laser frequency (homodyne interferometer) or two laser frequencies (heterodyne interferometer) with a difference in frequency Δf_{het}. This heterodyne frequency can be between 1 kHz and several MHz and offers better noise immunity than the homodyne measurement. Also, interferometers can use polarizing optics (as e. g. retarder waveplates, polarizing beamsplitters) or non-polarizing optics. Polarizing optics always suffer from leakage of the 'wrong' polarization in each optical path. This polarization mixing can limit the performance of the interferometer. They also have a temperature dependency which might not be suitable for space applications.

A homodyne interferometer utilizing non-polarizing optical components is set up at the University of Birmingham [4]. They demonstrated a noise level below $10^{-12}\,\mathrm{m}/\sqrt{\mathrm{Hz}}$ for frequencies > 10 Hz and work is currently under way to optimize their design with respect to the LISA low frequency measurement band.

2. HETERODYNE INTERFEROMETER

Here, we present an interferometer which is based on a design by Wu et al. [5]. It represents a heterodyne interferometer with two spatial-separated beams with frequencies f_1 and f_2, cf. the schematic shown in Fig. 2. The design of this interferometer is based on maximized symmetry between reference

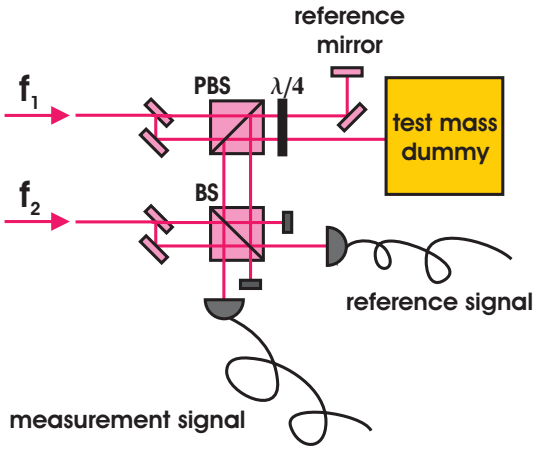

Figure 2. Schematic of the heterodyne interferometer (BS: beamsplitter; PBS: polarizing beamsplitter).

and measurement arm of the interferometer. Both have the same polarization and frequency. In front of the photodiode, they are superimposed with the second frequency in order to generate the heterodyne beat signal. This design also takes care that the optical paths of the reference and measurement arm are the same (i. e. same distances travelled in optical elements). Therefore, common-mode distortions and frequency noise are maximally rejected and polarization mixing is avoided.

With two laser frequencies f_1 and f_2 with amplitudes A and B, the measurement signal is given by $I_m \propto AB \cdot \cos(\Delta\omega t - \phi(t))$ and the reference signal by $I_r \propto AB \cdot \cos(\Delta\omega t)$. Here, $\Delta\omega = 2\pi \cdot |f_1 - f_2|$. The phase difference $\phi(t)$ on the measurement diode is proportional to the displacement Δl of the measurement mirror:

$$\phi(t) = \frac{4\pi n}{\lambda}\Delta l(t) \qquad (1)$$

with n the refractive index of the medium the light is travelling in.

In-quadrature measurement of the phase between I_r and I_m results in the two signals $S_1 = \frac{1}{2}AB\cdot\cos(\phi(t))$ and $S_2 = \frac{1}{2}AB \cdot \sin(\phi(t))$. The phase measurement is obtained via

$$\phi(t) = tan^{-1}\left(\frac{S_2}{S_1}\right) . \qquad (2)$$

3. DIFFERENTIAL WAVEFRONT SENSING

Alignment information – i. e. information on a tilt of the measurement mirror – can be obtained by replacing the single-element photodiode for the measurement signal by a position sensitive device, as e. g. a quadrant photodiode. The sum signal of the quadrant photodiode is used for the translation measurement. The wavefront reflected off the reference mirror is at all times plain while the wavefront reflected off the measurement mirror is tilted in case of a tilted measurement mirror. This tilt causes a non-uniform interferometer pattern across the quadrant diode. By comparing the phase of the signals of two opposite halves of the quadrant diode, an angular information can be obtained (two angles). This method is also utilized in the interferometer in the LISA Technology Package onboard LISA Pathfinder where a noise level of $\sim 10\,\mathrm{nrad}/\sqrt{\mathrm{Hz}}$ for frequencies $> 10^{-2}\,\mathrm{Hz}$ has been demonstrated [6].

4. COMPACT SETUP

As a first demonstrator, we realized a compact setup of the heterodyne interferometer design described above. The two frequencies are generated by use of one laser, whose output beam is split into two and each beam is frequency shifted by use of an acousto-optic modulator (AOM).

Our setup utilizes mechanically highly stable optical mounts with a beam height of only 2 cm. These mounts were developed in the framework of other projects currently under way at the Humboldt-university Berlin. The interferometer part is placed in a vacuum chamber in order to minimize air fluctuations and to provide a better temperature stability. The pressure in the chamber is below 10^{-2} mbar.

4.1. Heterodyne Frequency Generation

As light source, an NPRO-type Nd:YAG laser (by Laser Zentrum Hannover) with a wavelength of 1064 nm is used. The laser provides 200 mW output power, where a small fraction (~ 10 mW) is split off for use in the interferometer. The linearly polarized light is split by a non-polarizing beam splitter and each beam is shifted in frequency by use of an acousto-optic modulator (Crystal Technology, model 3080-125). As input beams for the interferometer serve the beams deflected in the first order Bragg reflection which are frequency shifted with respect to the incoming beam by the RF-frequency the AOM is driven by. In our case, the two AOMs are working with slightly different RF-frequencies (80 MHz and 79.99 MHz, respectively) resulting in a frequency difference of 10 kHz. As the interferometer needs a stable phase relation between the two frequencies, the RF-frequencies for the AOMs are generated by use of two frequency generators (SRS DS345) which are synchronized via their internal 10 MHz reference.

4.2. Interferometer Setup

The interferometer is placed on a 4 cm thick cast aluminum breadboard with a diameter of 23 cm. The schematic and a photograph of the setup are shown in Fig. 3. The light is fibre coupled and supplied to the interferometer breadboard inside the vacuum chamber by use of two fibre vacuum feedthroughs. The intensities are in the order of 0.5 mW at the fibre outputs. At a 6 mm thick glass plate with a small wedge in order to avoid etalon effects, 4% of each beam intensity is split off to monitor photodiodes. Their signals can be taken for intensity stabilization of the two laser beams (e. g. by a feedback loop activating the intensity of the RF-power of the AOMs). On the interferometer breadboard, each beam is again split into two at a beam separator cube, providing in each case two parallel output beams with a parallelism $< 2'$. By use of polarizing optics (polarizing beam splitter, PBS, combined with a quarter-waveplate, $\lambda/4$), a 90° incidence on the test mass can be realized without loss of intensity. The half-waveplate ($\lambda/2$) is needed as the beam separator cube requires p polarization. At the 50:50 nonpolarizing beamsplitter (BS), the second frequency coming from collimator 1 is superimposed with the two other laser beams. One quadrant photodiode (QPD1, provided by Silicon Sensor) is supplying the measurement signal while another quadrant photodiode of the same type (QPD2) is supplying the reference signal. QPD1 is also taken for the DWS measurement. The optical power is $\sim 100\,\mu$W at the measurement mirror and $\sim 200\,\mu$W at the quadrant diodes.

The measurement mirror – i. e. the LISA test mass dummy – is a gold mirror applied to a PZT tip-tilt actuator (PI S-340 with LVDT sensors). For translational movement, an additional high voltage PZT (provided by Piezomechanik) is placed between the gold mirror and the tip-tilt actuator. The tip-tilt actuator has a total tilt angle of 2 mrad with a resolution of 500 nrad and a reproducibility of $\pm 1\,\mu$rad over the whole tilt angle. The PZT by Piezomechanik has no closed-loop option and provides a total displacement of 13 μm by applying -200 V to 1000 V. Its hysteresis is clearly seen in the measurements.

4.3. Phase Measurement

An analog in-quadrature phase readout was implemented utilizing double balanced mixers as phase detectors. The scheme of the phasemeter is shown in Fig. 4. For the translation measurement, the sum signals of both quadrant diodes were first band pass filtered at the heterodyne frequency of 10 kHz, amplified (by use of AD524 amplifiers) and split (ZSC-4-2 by Mini-Circuits). These four signals are the input signals for the double balanced mixer (ZAD-8 by Mini-Circuits) where one LO mixer input signal

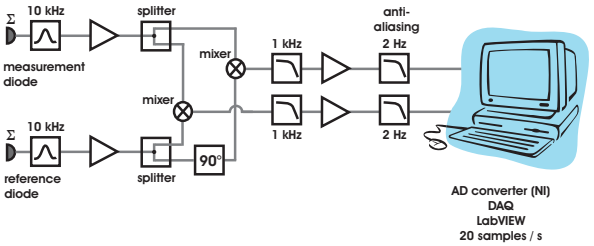

Figure 4. Schematic of the analog phase readout. For the translation measurement, the two input signals are the sum signals of the two quadrant diodes.

is shifted by 90° for obtaining the in-quadrature signal. The IF output signals of the mixers are low pass filtered, amplified and anti-alias filtered with a 6th order Bessel filter with a cut-off frequency of 2 Hz. The signals are digitized using a National Instruments 6229 M Series data acquisition board. A LabVIEW program calculates the arc tangent as given in Equation 2. In the interferometer a translation by $\lambda/2$ will cause the same signal where during the translation the arc tangent makes a jump by π. This jump is registered by the LabVIEW program offering a dynamic range not limited by $\lambda/2$.

The phase readout for the tilt measurement is similar to the readout for the translation measurement described above. Here, the input signals are the signals from two opposing quadrants. The arctangent is calculated by a LabVIEW program and the measured phase is converted to a tilt angle α of the measurement mirror via the conversion factor derived in [7], in our case 13500.

5. MEASUREMENTS

First measurements were done with the setup as described in Section 4 with the gold mirror glued to the PZT actuator as measurement mirror representing the LISA test mass. This configuration was used to test the in-quadrature phase readout. Translations over the dynamic range of the PZT were measured.

These measurements showed a temperature coefficient of ~ 1000 nm/K and a linear drift of ~ 100 nm/day which was not temperature correlated. In a setup where both, measurement beam and reference beam, were reflected off the same gold mirror attached to the PZT actuator, the temperature coefficient was reduced to ~ 25 nm/K.

As this environment is not suitable for testing the LISA requirement, the PZT actuator was removed. Now both, reference and measurement beam, were reflected off the same fix mirror. The power spectral density (PSD) of the translation noise is shown in Fig. 5 (blue line); Fig. 6 shows the PSD of the tilt measurement. Both graphs are shown for the LISA

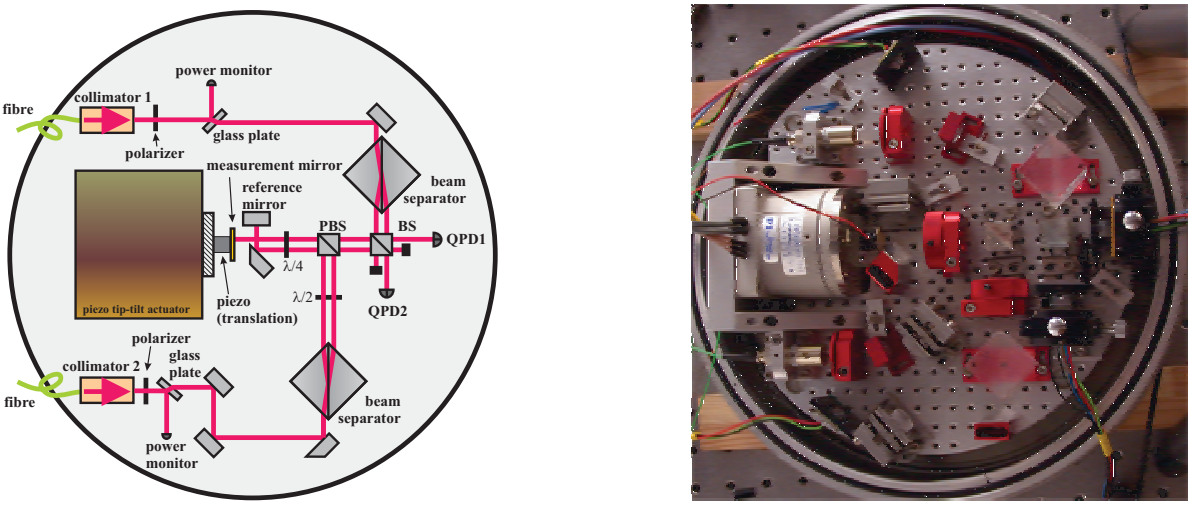

Figure 3. Left: Schematic of our setup (QPD: quadrant photodiode); Right: photograph of our interferometer setup in the vacuum chamber. The interferometer is placed on a 23 cm diameter aluminum breadboard.

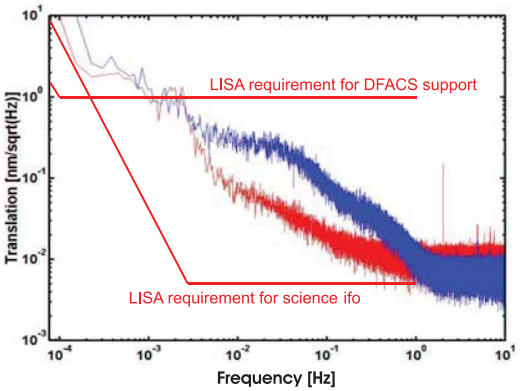

Figure 5. Measurement of the translation noise of the interferometer. Here, measurement and reference beam are both reflected by the same fix mirror.

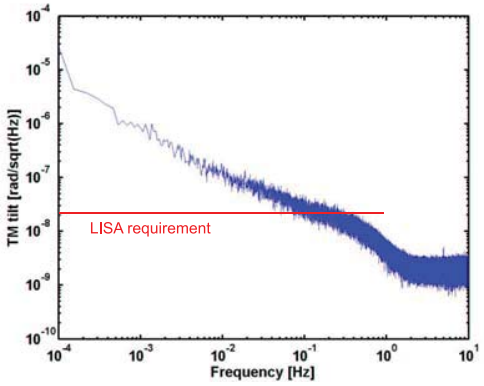

Figure 6. Measurement of the tilt noise of the interferometer where measurement and reference beam are both reflected by the same fix mirror.

measurement frequency band and the LISA requirements are included. For the translation measurement, the requirement depends on the LISA science interferometer design, cf. Section 1.

These measurements show a translation noise of $< 1\,\mathrm{nm}/\sqrt{\mathrm{Hz}}$ and a tilt noise of $< 1\,\mu\mathrm{rad}/\sqrt{\mathrm{Hz}}$ for frequencies $> 10^{-3}\,\mathrm{Hz}$. The PSD of the temperature in the vacuum chamber, converted to translation noise by the temperature coefficient of $\sim 25\,\mathrm{nm/K}$, is shown as red line in Fig. 5. Below $\sim 3 \cdot 10^{-3}\,\mathrm{Hz}$, our measurement is limited by temperature variations in the vacuum chamber. The noise level of about $10^{-2}\,\mathrm{nm}/\sqrt{\mathrm{Hz}}$ for frequencies $> 1\,\mathrm{Hz}$ corresponds to the digitizing noise of the 16 bit A/D-converter. The shot-noise corresponds to $\sim 0.1\,\mathrm{pm}/\sqrt{\mathrm{Hz}}$ and therefore states no limitation.

We also analyzed the two interferometer signals on the two quadrant diodes separately. These measurements show a huge common-mode signal and a common-mode-rejection performed by the differential phase measurement of about 150.

6. OUTLOOK

While the LISA requirement for the optical readout as DFACS support is fulfilled for the translation measurement, we need to gain one to two orders of magnitude in performance concerning the tilt measurement and the translation measurement where the optical readout is part of the LISA science interferometer. We therefore plan a new setup in a larger vacuum chamber with more space for diagnostics. In the new setup, part of the fibre outputs will be superimposed on a photodiode in order to implement

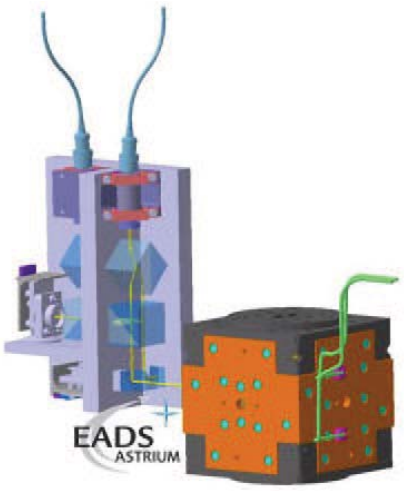

Figure 7. Sketch of a very compact, mechanically and thermally highly stable setup utilizing glass materials and hydroxide-catalysis bonding technology. The test mass with its housing is shown on the right.

a phase-lock of the heterodyne frequencies. All fibre effects will therefore be eliminated and the large common-mode signal will be decreased. Also, intensity noise and frequency noise of the laser and from the fibres will be analyzed in more detail. If necessary, an intensity stabilization (by feedback onto the RF-amplitudes of the AOMs) will be implemented. Additionally, our Nd:YAG laser can be frequency stabilized to molecular Iodine by use of modulation transfer spectroscopy [8]. Also, we will implement a digital phasemeter based on a National Instruments FPGA data acquisition board, directly digitizing the signals from the quadrant photodiodes.

We also plan a very compact and quasi-monolithic setup with improved temperature stability. Therefore fused silica optical components are connected to a baseplate out of a thermally stable glass material as e. g. Zerodur via hydroxide-catalysis bonding [9]. This technology is currently used for the LISA Pathfinder Optical Bench and fulfills requirements concerning space-qualification. A possible implementation of such a small fibre-coupled module is shown in Fig. 7.

7. SUMMARY

We presented a compact setup of a heterodyne interferometer as demonstrator of an optical readout for the LISA test mass position. First measurements show a translation noise of $< 1\,\mathrm{nm}/\sqrt{\mathrm{Hz}}$ and a tilt noise of $< 1\,\mu\mathrm{rad}/\sqrt{\mathrm{Hz}}$ for frequencies $> 10^{-3}\,\mathrm{Hz}$. For frequencies below $3 \cdot 10^{-3}\,\mathrm{Hz}$, our interferometer is limited by temperature variations in the vacuum chamber. The limitations above $3 \cdot 10^{-3}\,\mathrm{Hz}$ are under investigation. In a new setup, the heterodyne frequency laser beams will be stabilized in intensity. They will also be phase-locked in order to maximize common-mode suppression.

8. ACKNOWLEDGMENTS

The authors thank the Albert-Einstein-Institute Hannover for their cooperative support and fruitful discussions.

REFERENCES

1. F. Acernese, E. Calloni, R. De Rosa, L. Di Fiore, and L. Milano. An optical readout system for the drag-free control of LISA. *Class. Quantum Grav.*, 22:S279–S285, 2005.

2. E. Morrison, B. J. Meers, D. I. Robertson, and H. Ward. Automatic alignment of optical interferometers. *Appl. Opt.*, 33(22):5041–5049, 1994.

3. E. Morrison, B. J. Meers, D. I. Robertson, and H. Ward. Experimental demonstration of an automatic alignment system for optical interferometers. *Appl. Opt.*, 33(22):5037–5040, 1994.

4. C.C. Speake and S.M. Aston. An interferometric sensor for satellite drag-free control. *Class. Quantum Grav.*, 22:S269–S277, 2005.

5. C.M. Wu, S.T. Lin, and J. Fu. Heterodyne interferometer with two spatial-separated polarization beams for nanometrology. *Opt. Quantum Electron.*, 34(12):1267–1276, 2002.

6. G. Heinzel, C. Braxmaier, M. Caldwell, K. Danzmann, F. Draaisma, A. Garcia, J. Hough, O. Jennrich, U. Johann, C. Killow, K. Middleton, M. te Plate, D. Robertson, A. Rüdiger, R. Schilling, F. Steier, V. Wand, and H. Ward. Successful testing of the LISA technology package (LTP) interferometer engineering model. *Class. Quantum Grav.*, 22:1–6, 2005.

7. H. Müller, S.-W. Chiow, Q. Long, C. Vo, and S. Chu. Active sub-Rayleigh alignment of parallel or antiparallel laser beams. *Opt. Lett.*, 30:3323–3325, 2005.

8. T. Schuldt, C. Braxmaier, H. Müller, G. Huber, A. Peters, and U. Johann. Frequency stabilized Nd:YAG laser for space applications. In *Proceedings of the 5th International Conference on Space Optics (ICSO 2004)*, pages 611–617, ESA Publications, 2004.

9. E. J. Ellife, J. Bogenstahl, A. Deshpande, J. Hough, C. Killow, S. Reid, D. Robertson, S. Rowan, H. Ward, and G. Cagnoli. Hydroxide-catalysis bonding for stable optical systems for space. *Class. Quantum Grav.*, 22:S257–S267, 2005.